European **J**ournal of **Chem**istry

High thermal stability of aliphatic polyurethanes prepared from sesame and peanut oil and their kinetic parameters

Venkatesh Desappan and Jaisankar Viswanathan *

Department of Chemistry, Presidency College (Autonomous), Chennai-600005, India
venkatesh.d91@gmail.com (V.D.), vjaisankar@gmail.com (J.V.)

* Corresponding author at: Department of Chemistry, Presidency College (Autonomous), Chennai-600005, India.
 Tel: +91.9003248359 Fax: +91.044.28510732 e-mail: vjaisankar@gmail.com (J. Viswanathan).

RESEARCH ARTICLE

ABSTRACT

Thermo-responsive vegetable oil-based polyurethanes were successfully prepared by poly-condensation reaction in the mixture of polyol and hexamethylene diisocynate. The functionality and high molecular weight of the polyurethanes were characterized by Fourier Transform Infrared Spectroscopy (FTIR), Proton Nuclear Magnetic Resonance Spectroscopy (^{1}H NMR), Carbon Nuclear Resonance Spectroscopy (^{13}C NMR), and Gel Permeation Chromatography. The viscosity of the polyols was characterized by Rheometry and flow rate of the polyols were derived from power law model. The kinetic and thermodynamic parameters of synthesized polyurethanes HSCP and HPCP were calculated from by TG curve. Five different mass loss temperature was obtained in the TGA curve of HSCP and HPCP, which corresponded to the decomposition of the physically observed NH and C=O formed between polyol and diisocyanate, respectively. The average value of the activation energy calculated by Murray and White, Coats and Redfern, Doyle's, and Freeman-Carroll's method. The success of the investigated different vegetable oil-based polyurethanes, in comparison with the activation energy of the Freeman-Carroll's method to determine the thermal stability and the lifetime prediction of the peanut and sesame oil-based polyurethanes is 1.87×10^5 and 1.27×10^4 s^{-1}.
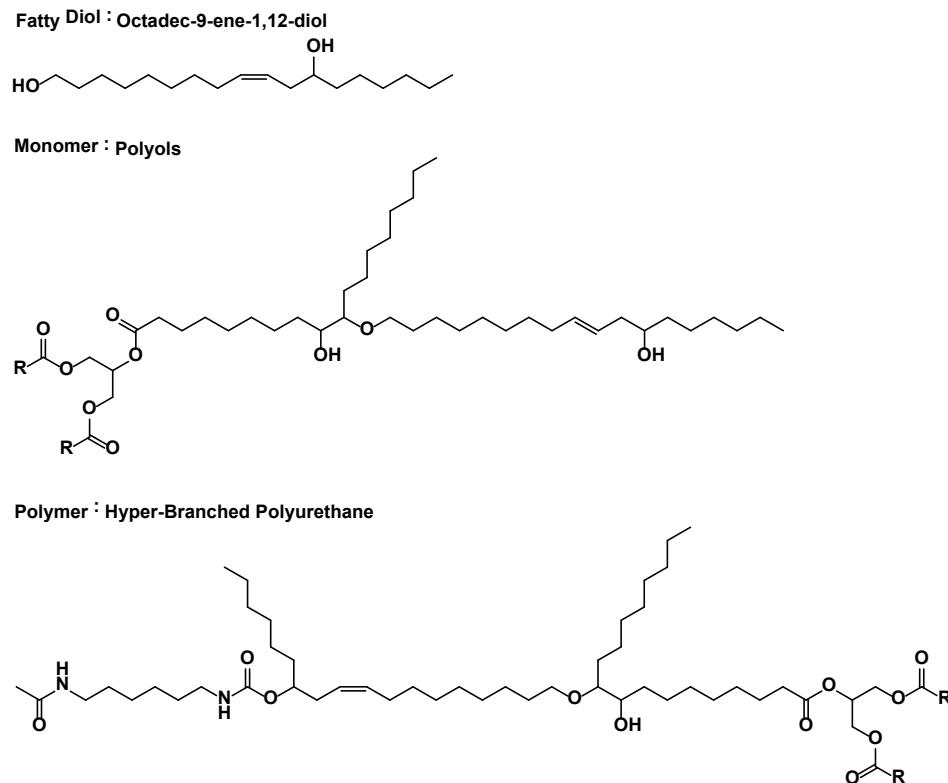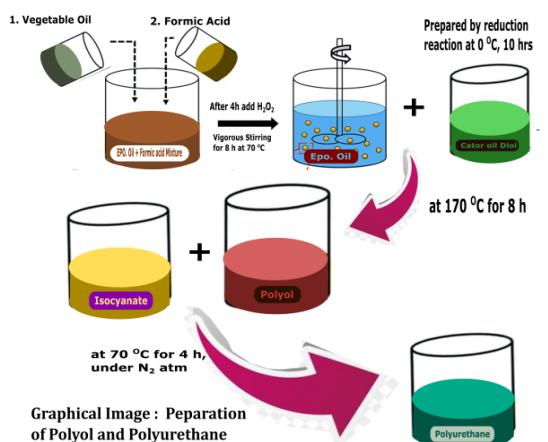
Journal website: www.eurjchem.com

1. Introduction

Vegetable oil-based polyols possess a high molecular weight and a considerable degree of reactive branching. They are multifunctional starting materials consists of mainly heterogeneous triglyceride structures which enable chemists to design polymers for different applications (Scheme 1) [1]. Vegetable oils usually offer two major reactive sites for their conversion into polyols. The polyols are obtained either by direct polymerization or by functionalization of the oil through double bond reactions such as epoxidation, hydro-formylation, and metathesis, or through ester bond-breaking reactions. Polyols may be prepared by direct oxidation of the double bonds present in vegetable oils, which contain sufficient unsaturation. The epoxidation of vegetable oil is carried out on an industrial scale to obtain a variety of polyols [1,2]. Hence, the epoxidation is one of the most important functionalization reactions of the carbon-carbon double bond of fatty acids of vegetable oils. This functionalization can be achieved through environmentally friendly procedures, such as (i) epoxidation with peracids such as perbenzoic acid in the presence of an acid catalyst; (ii) epoxidation with organic and inorganic peroxides, including transition metal catalysts; (iii) epoxidation with halo-hydrins using hypohalous acids and their

salts and (iv) epoxidation with molecular oxygen. The oxirane ring is split by halo-acids and diol to obtain halogenated and functionalized polyols [1-3]. Several aspects like the progress of the reaction, the type of catalyst, alcohol to vegetable oil mole ratio, temperature, and free fatty acid content, have an influence on the final product. Vegetable oil polyol and different diisocyanates which are used to prepare aliphatic and aromatic polyurethanes [4,5]. The properties of polyurethanes also depend on the structure of the isocyanate component (Scheme 1). Among, the most common diisocyanates used on a large scale are hexamethylene diisocyanate (HMDI) [6]. The reactivity of aliphatic diisocyanates is lesser than in aromatic diisocyanates. The rigidity of the polyurethane network and the enhancement of most properties are found to be in the order, aromatic > cycloaliphatic > aliphatic diisocyanates. HMDI are the two most common commercially used aliphatic diisocyanates. Furthermore, the aliphatic diisocyanates such as hexamethylene diisocyanate and isophorone diisocyanate (IPDI) are comparatively more reactive and produce poly-urethanes with high strength and thermal stability [7,8]. The aliphatic diisocyanate-based polyurethanes possess superior retention of modulus, hydrolysis, resistance to water uptake, hardness, hydrolysis, and high thermal degradation compared to aromatic diisocyanate-based polyurethanes [1,7-13].

Fatty Diol : Octadec-9-ene-1,12-diol

Monomer : Polyols

Polymer : Hyper-Branched Polyurethane

Scheme 1. Structure of polyols and polyurethanes.

Figure 1. Preparation of polyols and polyurethanes.

Hence aliphatic diisocyanates find a wider use in elastomer and coating applications where color is an important consideration than their aromatic counterparts [14-19].

This investigation deals with the epoxidized oil ring opening is an important class of organic equilibrium exchange reaction in which one epoxy ring opened by another castor diol. The preparation method follows a variety of vegetable oils such as castor oil diol (CaOD) was used to ring-opening of epoxy groups in epoxidized sesame oil (ESO), epoxidized peanut oil (EPO) (Figure 1). Also deals with synthetic and thermal degradation properties of a newly synthesized polyol and aliphatic linked polyurethane (PUs) characterized by thermal gravimetric analysis (TGA). The kinetics of thermal degradation studies has been discussed with thermal degradation properties were discussed and analyzed from TGA curve.

Since, the thermal degradation curve analyzed in Freeman-Carroll method order to determine their mode of decomposition, an order of reaction and lifetime prediction. The activation energy of the polyurethane was calculated from Murray and White, Coat's and Redfern, Doyle's method. Freeman-Carroll's method has been applied for the calculation of pre-exponential factor, enthalpy, entropy, apparent entropy, frequency factor, free energy change, and order of reaction. The lifetime prediction of the polymers calculated from the apparent activation energy, which is calculated from Freeman and Carroll's method. Based on the order of the reaction and apparent activation energy helpful to predicting the lifetime of the sesame and peanut oil-based polyurethanes.

2. Experimental

2.1. Materials

Vegetable oils such as sesame, peanut, (approximately six oxirane rings per triglyceride) were purchased from a local source. Magnesium sulfate, hydrogen peroxide, methyl ethyl ketone (MEK), hexamethylene diisocyanate (HMDI) and ethyl ether were purchased from Fisher Scientific Company (Fair Lawn, NJ). Hydrochloric acid, sodium hydroxide, sodium bicarbonate, formic acid and dibutyltin dilaurate (DBTDL) were obtained from Sigma-Aldrich (Milwaukee, WI). All materials were used without further purification.

2.2. Synthesis of vegetable oil

2.2.1. Synthesis of the epoxidized vegetable oils

Epoxidized vegetable oils with different epoxy groups were prepared according to a method previously reported [4,5]. Briefly, sesame oil and formic acid (the molar ratio of these two is 1:4.12) were charged into a 500 mL flask at 50 °C under vigorous stirring. Then, hydrogen peroxide (50%, the molar ratio of hydrogen peroxide to double bonds in triglyceride is 1.8:1) was added slowly using syringe over 4 h period. The reaction was continued at 50 °C for another 4 h. Then, sodium bicarbonate was added to neutralize the solution and diethyl ether was added, resulted in two layers. The organic layer was washed with distilled water until the solution became neutral. Epoxidized sesame oil was obtained after drying with MgSO₄ and filtered. The organic solvent is removed by rotary evaporator, and the product was dried in a vacuum oven overnight. The same procedure was followed for the synthesis of epoxidized peanut oil.

Epoxidized sesame oil (ESO): Color: Yellowish brown. Yield: 73 %. FT-IR (KBr, ν, cm⁻¹): 828 *ν*(Epoxy group), 1367 *β*(C-H), 1743 (C=O).

Epoxidized peanut oil (EPO): Color: Brown. Yield: 70%. FT-IR (KBr, ν, cm⁻¹): 833 *ν*(Epoxy group), 1382 *β*(C-H), 1732 (C=O).

2.2.2. Synthesis of octadec-9-ene-1,12-diol

CaOD was prepared using a reported procedure [5]. Firstly, 100 mL of THF was added to LiBH₄ in a 1000 mL three-neck flask at 0 °C. Then, the addition of castor oil 0.11 mol was dissolved in THF and then added to the LiBH₄ suspension with mechanical stirring. The reaction was maintained at 0 °C for 10 hrs. The reaction mixture was poured into a 2000 mL bleak with ice water, followed by addition of HCl, until the solution was clear. After the extraction with 300 mL of ethyl acetate, the organic layer was purified by washing with water, drying over MgSO₄, and filtering. Finally, the clear castor oil diol was obtained after removal of organic solvent using rotavapor and dried under vacuum. Chain Extender (CaOD): Color: Dark brown. M.p.: 185-191 °C. Yield: 92 %. FT-IR (KBr, ν, cm⁻¹): 3479 (-OH), 1395 (C=C).n¹H NMR (400 MHz, CDCl₃, δ, ppm): 5.52 (dd, *J* = 10.7, 6.0 Hz, 7H), 5.06 (dd, *J* = 208.1, 121.3, 60.4 Hz, 12H), 5.05-3.54 (m, 24H), 4.70-3.13 (m, 22H), 4.70-3.54 (m, 22H), 2.45 (t, *J* = 120.2 Hz, 17H), 2.45 (t, *J* = 120.2 Hz, 16H), 2.53-2.10 (m, 42H), 1.62 (s, 26H), 1.52 (d, *J* = 9.8 Hz, 15H), 1.48-1.10 (m, 209H), 2.10- -1.83 (m, 335H), 1.82- -1.83 (m, 313H), 1.10-0.99 (m, 5H), 0.89 (d, *J* = 3.0 Hz, 35H), 0.78- -3.97 (m, 16H).

2.2.3. Synthesis of 9-hydroxy-10-(12-hydroxy-octadec-9-enyloxy)-octadecanoic acid 1-[10-hydroxy-9-(12-hydroxy-heptadec-9-enyloxy)-octadecanoyloxymethyl]-2-[10-

hydroxy-9-(11-hydroxy-octadec-9-enyloxy)-octadecanoyl oxy]-ethyl ester

The polyols were prepared by the ring-opening reaction previously reported R.C. Kessler *et al.* [4,5]. The sesame-castor and peanut-castor oil polyols prepared from epoxidized oil were rings opened by modified castor oil diol. The polyols were prepared by solvent/catalyst free method. Furthermore, the synthesized polyols were identified as namely SCOL and PCOL. Several aspects, the castor oil diol and epoxidized oil (ESO) were mixed and kept at 65 °C in the dry N₂ atmosphere. After the 8 hours, a brown-yellowish viscous liquid (SCOL) was obtained. The same procedure was followed to prepare another polyol (PCOL).

Monomer (Polyol, SCOL): Color: Dark brown. M.p.: 189-194 °C. Yield: 84 %. FT-IR (KBr, ν, cm⁻¹): 3498 (OH), 1018 (C-O-C), 1367 (bending C-H), 1335 (C=C). ¹H NMR (400 MHz, CDCl₃, δ, ppm): 5.61-5.17 (m, 21H), 4.41-3.86 (m, 15H), 3.70-3.47 (m, 3H), 2.73 (dt, *J* = 25.4, 13.0 Hz, 4H), 2.40-2.20 (m, 35H), 2.14-1.86 (m, 27H), 1.80-1.46 (m, 39H), 1.28 (d, *J* = 23.0 Hz, 220H), 1.12-0.64 (m, 265H), 0.30 (t, *J* = 6.2 Hz, 36H). ¹³C NMR (100 MHz, CDCl₃, δ, ppm): 173.48 (d, *J* = 22.9 Hz), 173.03-172.62 (s)(CO triglyceride carbonyl), 129.54-130.02 (s) (C=C), 76.95 (s) (for triglyceride HC-OH), 71.44 (s)(for chain extender HC-OH), 14.11-13.78 (m) (terminal CH₃), 68.87 (s), 64.83(s), 61.98(s), 36.65(s), 35.16(s), 34.48 (s), 34.30-33.56 (m), 33.48 (d), 32.47 (d), 32.09-31.52 (m), 31.41 (s), 29.79-28.25 (m), 27.15 (dd), 25.55 (d), 25.19 (d), 24.97 (s), 24.73 (d), 22.68-22.35 (m) internal carbon chain of monomer. GPC (PDI value n > 1): 1.54.

Monomer (Polyol, PCOL): Color: Brown. M.p.: 189-194 °C. Yield: 88%. FT-IR (KBr, ν, cm⁻¹): 3462 (OH), 1023 (C-O-C), 1382 (bending C-H), 1364 (C=C). ¹H NMR (400 MHz, CDCl₃, δ, ppm): 5.61-5.17 (m, 21H), 4.41-3.86 (m, 15H), 3.70-3.47 (m, 3H), 2.73 (dt, *J* = 25.4, 13.0 Hz, 4H), 2.40-2.20 (m, 35H), 2.14-1.86 (m, 27H), 1.80-1.46 (m, 39H), 1.28 (d, *J* = 23.0 Hz, 220H), 1.12-0.64 (m, 265H), 0.30 (t, *J* = 6.2 Hz, 36H). ¹³C NMR (100 MHz, CDCl₃, δ, ppm): 173.48 (d, *J* = 22.9 Hz), 173.03-172.62 (s)(CO triglyceride carbonyl), 129.54-130.02 (s) (C=C), 76.95 (s) (for triglyceride HC-OH), 71.44 (s)(for chain extender HC-OH), 14.11-13.78 (m) (terminal CH₃), 68.87 (s), 64.83(s), 61.98(s), 36.65(s), 35.16(s), 34.48 (s), 34.30-33.56 (m), 33.48 (d), 32.47 (d), 32.09-31.52 (m), 31.41 (s), 29.79- 28.25 (m), 27.15 (dd), 25.55 (d), 25.19 (d), 24.97 (s), 24.73 (d), 22.68-22.35 (m) internal carbon chain of monomer. GPC (PDI value n > 1): 1.36.

2.2.4. Synthesis of polyurethane

The synthesized polyol SCOL were reacting with 0.5% excess of hexamethylene diisocyanate (HMDI) to prepare (HSCP) polyurethane. Ethylmethylketone (MEK) used as a solvent under 70 °C at N₂ atmosphere. The same procedure was followed to prepare other polyurethane such as HPCP.

HSCP: Color: Pale yellow. Yield: 81%. FT-IR (KBr, ν, cm⁻¹): 3324 (str. NH), 1707 (non-hydrogen bonded >C=O), 1638 (hydrogen bonded C-O-), 1718 (symmetrical stretching disordered hydrogen- bonded C=O), 1225 (-NH-C-O-), 1588 (N-H bending vibrations). ¹H NMR (400 MHz, DMSO-*d₆*, δ, ppm): 8.64-7.45 (m, 49H), 7.27 (dd, *J* = 65.4, 53.8 Hz, 112H), 7.10-6.76 (m, 90H), 6.48 (d, *J* = 8.0 Hz, 10H), 5.30 (s, 17H), 5.16-4.95 (m, 8H), 4.84 (s, 23H), 4.77-4.21 (m, 53H), 3.74 (d, *J* = 62.3 Hz, 58H), 3.33 (s, 249H), 2.64 (s, 4H), 2.51 (s, 165H), 2.43 (dd, *J* = 14.6, 7.3 Hz, 11H), 2.37 (s, 5H), 2.26-2.22 (m, 10H), 2.02 (d, *J* = 56.9 Hz, 52H), 1.64 (s, 30H), 1.50-0.62 (m, 393H), 0.62- (-0.84) (m, 99H), (-0.84)-(-1.43) (m, 26H). GPC (PDI value n > 1): 1.74.

HPCP: Color: Dirty white. Yield: 77%. FT-IR (KBr, ν, cm⁻¹): 3314 (stretching -NH), 1711 (non-hydrogen bonded >C=O), 1643 (hydrogen bonded C-O-), 1720 (symmetrical stretching
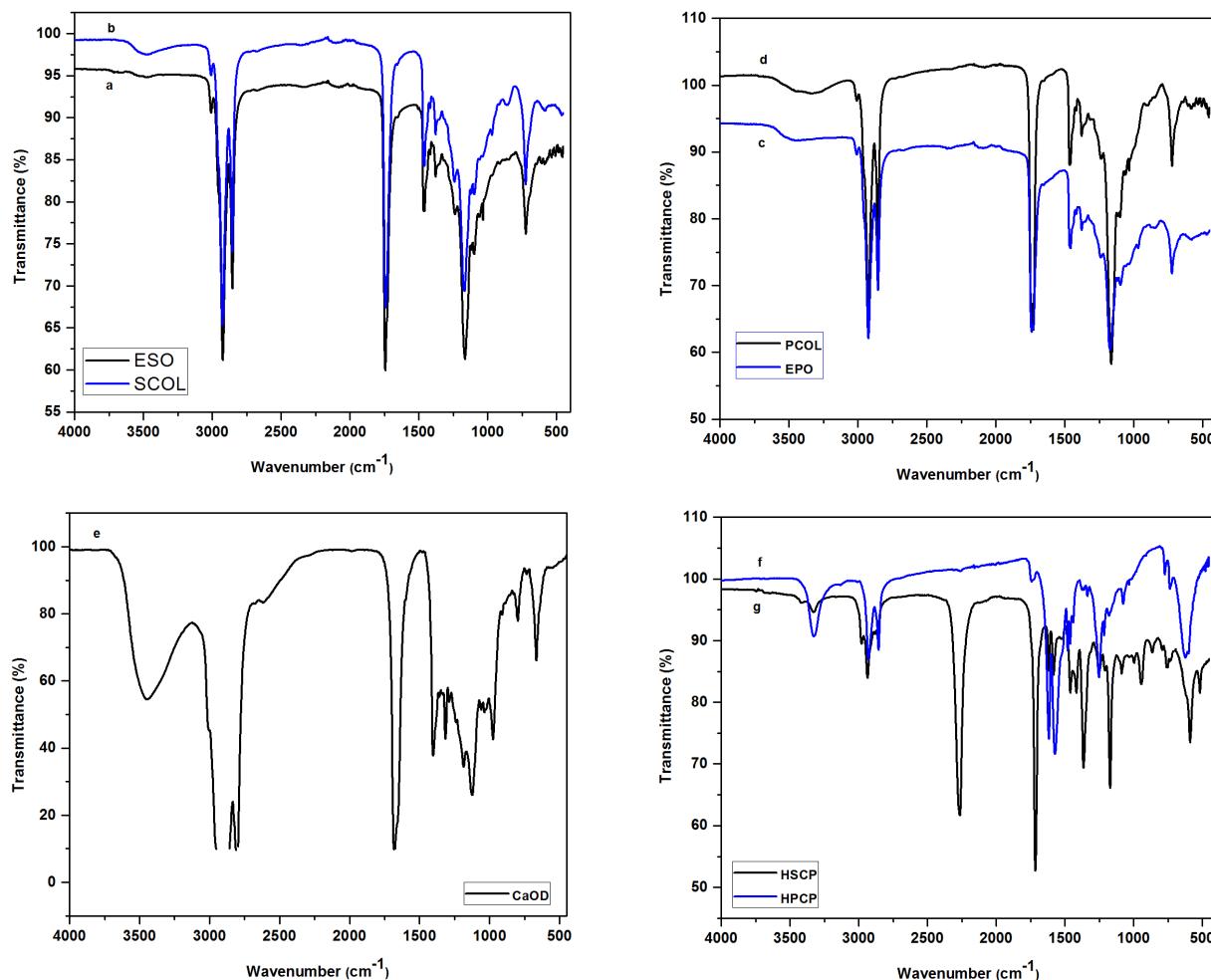
Figure 2. FT-IR spectrum of (a) Epoxidized ESO oil, (b) SCOL polyol, (c) Epoxidized EPO oil, (d) PCOL polyol, (e) CaOD Diol, (f) HPCP polymer and (g) HSCP polymer.

disordered hydrogen- bonded C=O), 1322 (-NH-C-O-), 1598 (N-H bending vibrations). ^{1}H NMR (400 MHz, DMSO-d_6, δ, ppm): 8.64-7.45 (m, 49H), 7.27 (dd, J = 65.4, 53.8 Hz, 112H), 7.10-6.76 (m, 90H), 6.48 (d, J = 8.0 Hz, 10H), 5.30 (s, 17H), 5.16-4.95 (m, 8H), 4.84 (s, 23H), 4.77-4.21 (m, 45H), 3.74 (d, J = 62.3 Hz, 58H), 3.33 (s, 249H), 2.64 (s, 4H), 2.51 (s, 165H), 2.43 (dd, J = 14.6, 7.3 Hz, 11H), 2.37 (s, 5H), 2.26-2.22 (m, 10H), 2.02 (d, J = 56.9 Hz, 52H), 1.64 (s, 30H), 1.50-0.62 (m, 393H), 0.62-(-0.84) (m, 99H), (-0.84)-(-1.43) (m, 26H). GPC (PDI value n > 1): 1.90.

2.3. Characterization methods

Variant spectrometer chemical structural studies were conducted using Bruker FTIR analyzer; ALPHA-Platinum FT-IR Spectrometer with ATR Platinum-Diamond sampling module. A Varian spectrometer (Palo Alto, CA) at 400 MHz was used to record the ^{1}H and ^{13}C NMR spectroscopic analyses of the monomers of polyol and cross-linker CaOD diol. The prepared polyols and CaOD diol molecular weight distribution were measured using a Varian PL-gel permeation chromatography (GPC) 50 plus equipped with a differential refractive index (DRI)/viscometer, which is a combined detector. The reference material tetrahydrofuran (THF) used as a eluent and the flow rate was fixed 1.00 mL/min. The viscosity of prepared polyols was determined using U/S portable rheometer at 25 °C. Accurately weighed powder was taken into a pre-cleaned

platinum pan, heated at a programmed rate of 10 °C/min in the temperature range from 25 to 600 °C under nitrogen gas flow kinetics of thermal degradation studies has been discussed with synthetic and thermal degradation properties of a newly synthesized polymers derived from sesame oil polyol, peanut oil polyol and hexamethylene diisocyanate. Thermal degradation curve analyzed in order to determine their mode of decomposition, the order of reaction. The methods employed are Murray and White, Coats and Redfern, Doyle's and Freeman-Carroll methods have been applied for the calculation of activation energy), and pre-exponential factor, frequency factor, free energy change, entropy change, enthalpy, apparent entropy, lifetime prediction and order of reaction calculated from Freeman-Carroll's method.

3. Results and discussion

3.1. Fourier transform infrared spectroscopy

In this part, the prepared epoxy of vegetable oils and CaOD based different polyols structure and functionalities were investigated by FT-IR. The measurement of FT-IR was carried out in attenuated total reflectance mode using a Thermo Scientific Nicollet 6700 spectrometer. IR spectra were obtained at 4 cm^{-1} resolution between standard wave number ranging from 400 to 4000 cm^{-1} [1-5]. Figure 2a and 2c shows the FT-IR spectra of epoxidized ESO and EPO.
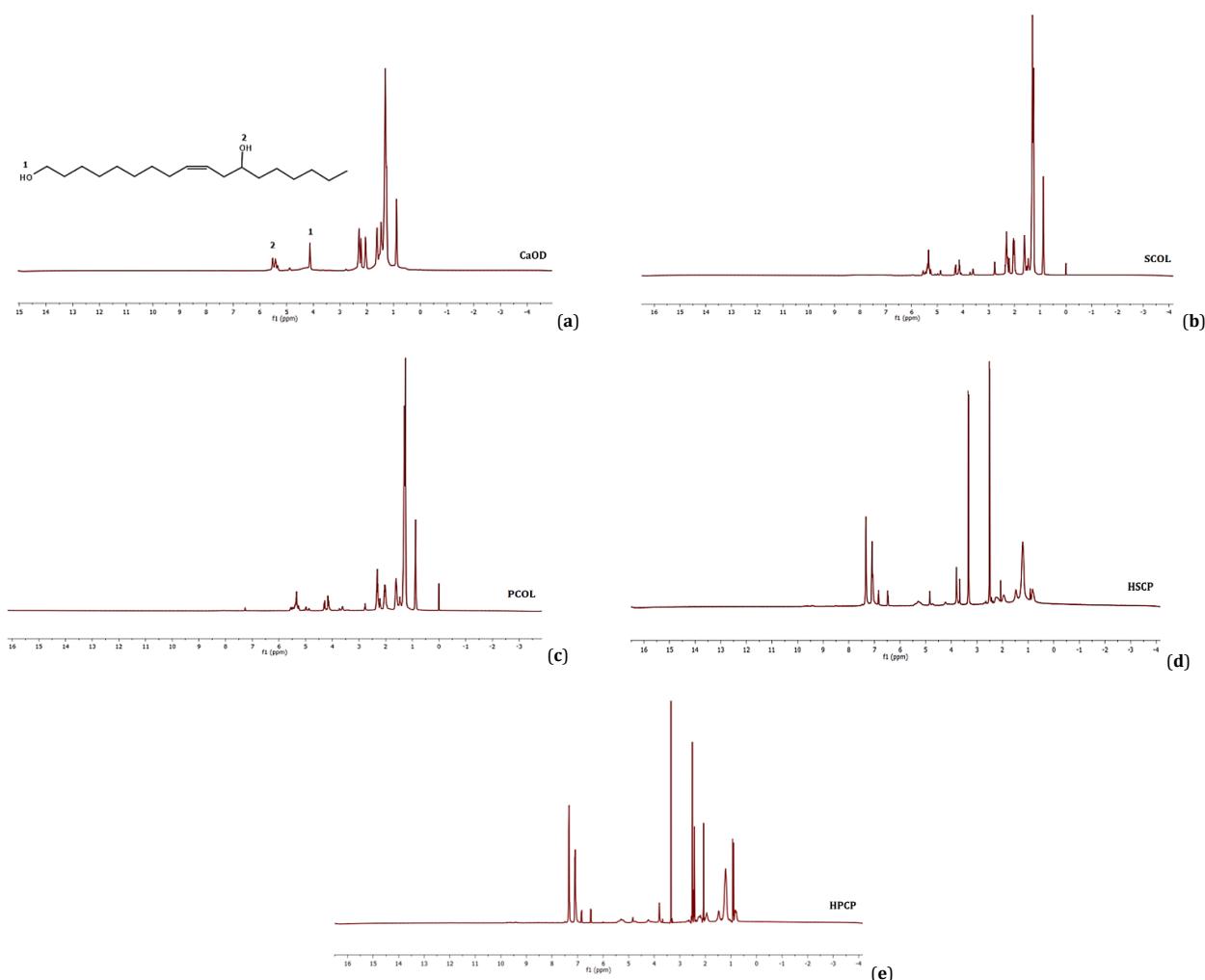
Figure 3. ^{1}H spectra of (a) CaOD fatty acid, (b) SCOL polyol, (c) PCOL polyol, (d) HSCP polymer and (e) HPCP polymer.

The FT-IR spectra reveal that the presence of epoxy group at 828 and 833 cm^{-1}, respective epoxy oils. Figure 2e shows, the broad peak between 3600 to 3000 cm^{-1}, which was assigned to the overlapped signal from the OH stretching of the hydroxyl group of the castor diol. The peak at 828 cm^{-1} was no longer observed for the diol because most of the epoxy groups were reduced during the ring opening step [4]. Figure 2b and 2d shows the intensity of epoxy group at 828 and 833 cm^{-1} are disappeared while CaOD of diol unit facilitates the ring opening of all the epoxy oils. The reaction of primary hydroxyl to epoxy group ratio was increased because of which shows that most of the epoxy groups were ring-opened by castor diol. The secondary-OH group is intrinsically present in the ricinoleic moiety of CaOD diol is shown in Scheme 1. On the other hand, the SCOL and PCOL polyol of all the OH groups, the presence of broad peak appeared at 3498 and 3462 cm^{-1} shows the primary and secondary OH group of CaOD overlapped with all the epoxy vegetable oils [4-6].

Fourier transformed infrared spectra of Figure 2f and 2g shows polyurethane HPCP and HSCP polymer are on the oxygen atoms of the carbonyl (>C=O), ether and ester group (C-O-C) and amine functional groups (C-N and N-H) absorbed at 1750-1710, 1300-1000 and 1550-1500 cm^{-1}. After the poly-condensation reaction the spectra of polyurethane, the >C=O stretching have three peaks due to free or non-hydrogen-bonded >C=O peak observed at 1727-1735 cm^{-1}, the

disordered hydrogen-bonded >C=O symmetrical stretching at 1718-1721 cm^{-1} and the vibrational stretching frequency observed at 1703-1704 cm^{-1}, respectively. On the other hand, it is valuable to mention the >N-H group in polyurethane could develop hard segment to hard segment disordered hydrogen bonding with the oxygen of carbonyl groups [7]. Such strong H bonding acts as physical cross-links leading to restrict the segmental motion of the polymer chain. The observed >N-H bending vibrations at 1598 cm^{-1}, C-O-C stretching absorption band corresponding to a linkage between -OH and -NCO groups to form urethane bond in the range 1057-1130 cm^{-1} also provide strong evidence for the formation of poly-urethanes. The peaks corresponding to the absorption of >NH, >C=O and >C-O- were observed at 3314, 1707 (non-hydrogen bonded), 1643 (hydrogen bonded) and 1225 cm^{-1}, respect-tively, which indicate the newly synthesized product having urethane (-NH-C-O-O) group.

3.2. Nuclear magnetic resonance spectrometry

The proton NMR of the polyols was prepared from ESO and EPO oils, ring opened by CaOD solvent free/catalyst-free method. Figure 3a shows the ^{1}H NMR spectra of CaOD diol, increasing their peak intensity at δ 5.3-5.4 ppm corresponding to carbon-carbon double bond in CaOD, the terminal -CH$_3$ and internal long chain protons of -CH$_2$- signal at δ 0.89 ppm and δ 1.63 ppm [4-6].
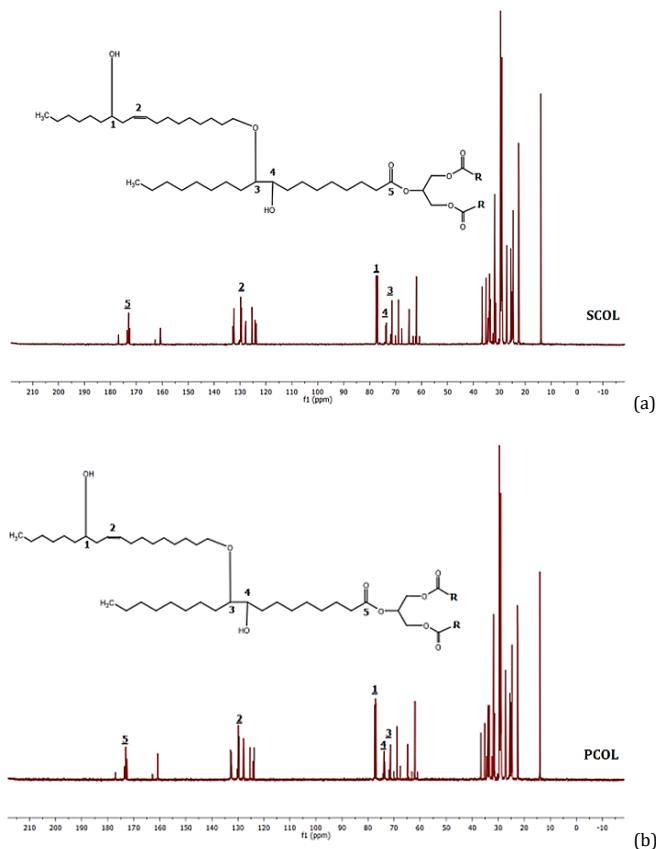
Figure 4. ^{13}C spectra of (a) SCOL polyol and (b) PCOL polyol.

The overlapped peaks for primary and secondary –OH protons of ricinoleic moiety appeared at 4.16 ppm [4-10].

The prepared SCOL and PCOL is shown in the Figure 3b and 3c. The chemical shift value observed at δ 2.21 ppm corresponds to the –CH$_2$C(O)O- proton. After the reduction reaction, the epoxy peak at δ 2.22-2.65 ppm disappeared [4-6,10]. The chemical shifts value of the methylene proton of ricinoleic acid (>C-C< double bond) signal shifted to δ 3.73 ppm. The intensity of the proton of >C=C< present in SCOL and PCOL were slightly decreased, because of the oxirane ring opened by castor diol (CaOD), obtained peak at δ 5.56 ppm. The ricinoleic of OH group overlapped with newly formed OH peak, the corresponding peak at δ 5.56 ppm [11]. On the other hand, the peak intensity at δ 4.5-4.6 ppm decreased, indicates the complete reduction of triglyceride. It results in the formation of primary OH groups backbone appears at δ 5.56 ppm [4]. It leads to the conclusion that SCOL and PCOL were successfully prepared and confirmed [12,13].

^{13}C NMR spectra of polyol SCOL and PCOL were shown in the Figure 4a and 4b. The chemical shifts value of –C-O-C< observed at δ 172 and δ 174 ppm. The corresponding methylene (>C=C<) peak appeared at δ 131 ppm, and the terminal and long-chain carbon give a signal at δ 14.0 ppm. After the ring opening of the oxirane ring, the signals obtained at δ 71, 34 and 27 ppm corresponds to carbon atoms of -C-C-C=C-C-, respectively. Finally, after the reduction reaction, the diol of CaOD secondary hydroxyl (-OH) group overlapped with newly formed –OH group, the obtained peak at δ 74 ppm, the corresponding >C-O-C-*C*H$_2$- peak at δ 32 ppm longer observed [5-13]. It concludes that the SCOL and PCOL were successfully prepared and again confirmed.

^{1}H NMR spectra of polyurethanes, the synthesized polyols (SCOL and PCOL) reacts with diisocyanates namely HMDI shown in Figure 3d and 3e. After the polycondensation reac-

tion the intensity of polyol peak δ 5.31 ppm decreased, and the new signal of urethane (>NH) was shown at HSCP and HPCP δ 8.53 and 8.24 ppm, other peaks observed at δ 7.00-7.10 ppm for HN-C=O, and observed peak at δ 3.64 ppm and δ 3.43 ppm designated to the protons of -CH$_2$OCO support the synthesis of polyurethane the polyols (SCOL and PCOL). The other peaks observed were assigned to a C=C proton as δ 5.18 ppm respectively [7,9-15].

3.3. Gel permeation chromatography

The GPC curve of polyol SCOL, PCOL were shown in Figure 5. The reaction of carboxyl to epoxy group ratio increases [4,5], the epoxy group were totally ring opened by CaOD [4,6,13-17]. From GPC curve, comparison of CaOD diol with SCOL and PCOL, Kessler *et al.* [5,19] and Petrovic *et al.* [13] discussed with GPC curve of the polyols, the intensity of the peaks corresponds to shorter and then longer retention time which take place the polyols have higher molecular weight) initially, the polyol retention peaks were shifted to longer retention time and became broadened, which indicates that the molecular weight of the polyol increased.
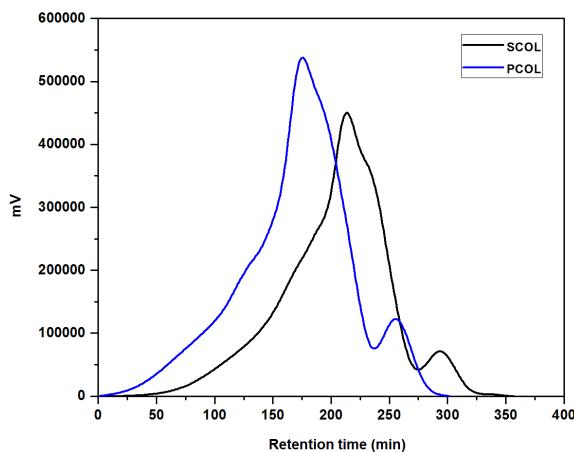
From this discussion, the obtained second peak shifted to shorter retention time. Considering there is another one secondary -OH group in CaOD, which the number was almost identical with the primary hydroxyl group. It is deduced that the -OH group in CaOD, as well as newly formed OH in epoxies, were also involved in the ring opening reaction and possibly connected with ESO and EPO monomers, leading to increasing molecular weight [15-18]. The molecular weight values are shown in Table 1. This can be explained, all the epoxidized vegetable oils fully ring opened by CaOD diol.

Table 1. Molecular weight of the monomer and polymers data.

Sample	Viscosity (pa s) 25 °C	Number average molecular weight ($\overline{Mn}$)	Weight average molecular weight ($\overline{Mw}$)	Polydispersity index
Polyol				
SCOL	0.50	1327	2056	1.54
PCOL	0.58	940	1279	1.36
Polyurethane				
HSCP	-	1500	1717	1.74
HPCP	-	1439	1592	1.90

Table 2. Flow rate of the polyol and castor diol calculated from Ostwald-de Waele power law model.

Sample	K (Pa s) 25 °C	n (-)	r^2
Polyols			
SCOL	1.023	0.2381	0.9997
PCOL	1.044	0.2539	0.9989
Castor Diol			
CaOD	1.671	0.5855	0.6901

Figure 5. GPC curve of SCOL and PCOL polyols.

3.4. Rheometry analysis

The viscosity of prepared polyols was determined by using R/S portal Rheometer at 25 °C for the shear rate varying from 1 to 100 s^{-1}. The polyols SCOL, PCOL and CaOD fatty acid plots (variation of shear stress against shear rate and viscosity against shear rate) shown in the Figure 6a-c. However, the Figures shows, the linear dependence of shear rate on shear stress.

Rheological experiments showed that all liquid samples tested were Newtonian fluids in the full range of shear rates investigated in the present work. As mentioned before the shear viscosity measurements of the polyol viscosities were carried out at 25 °C. The shear viscosities were also determined for several shear rates in order to investigate the possibility of shear rate viscosity dependence (i.e. a shear thinning behavior of the polyol). Mentioned above the figures with cross line shows the typical Newtonian behavior of the polyol, shear stress for the range of shear values explored and the values became quite independent of the shear rate. All values of shear stress presented this plot was obtained for a sufficiently long time of the experiment so that the viscous meter system reached the steady state and the shear stress saturated for the constant valued 25 °C for all shear rate tested [1-3,19]. Figures with horizontal line was plotted the polyols and diols, shear viscosity versus the shear rate at constant temperature (25 °C). Their results are for the condition in which the polyol is free of humidity. The sesame-castor and peanut-castor polyol and castor diol flow rate can be calculated from power law model, which can be determined the fluid behavior of each sample shown in Table 2. The power law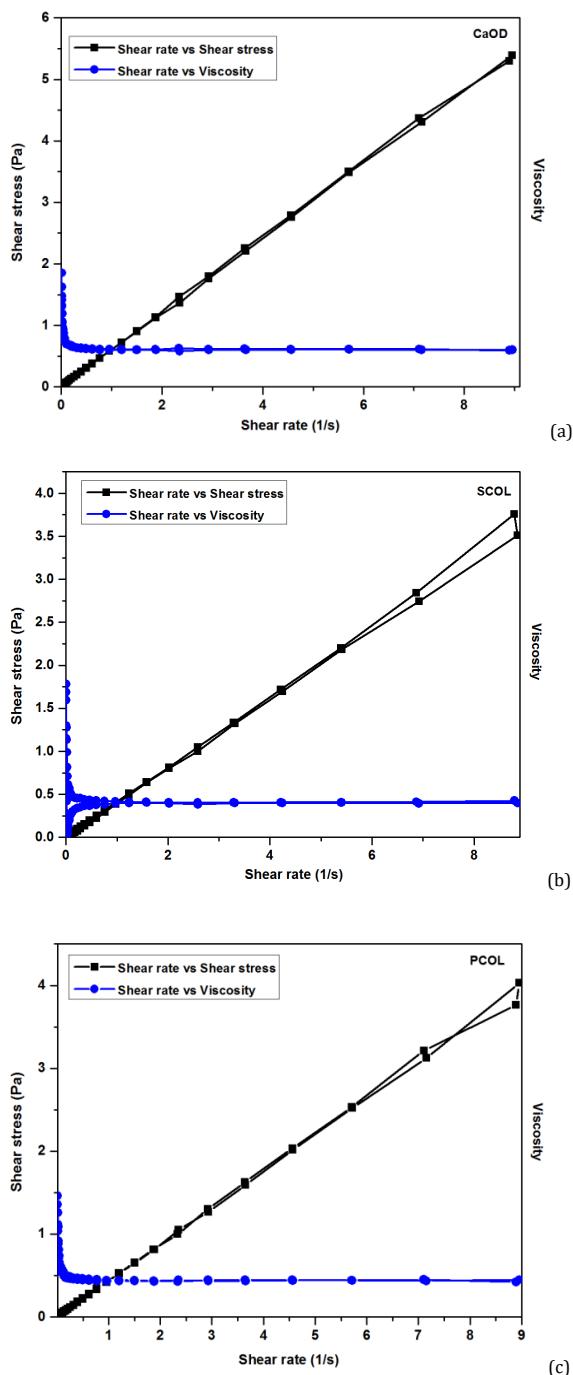 method had a flow behavior index n > 1, the obtained bio-polyols were "n" (order of flow behavior) value decreases and "K" (viscosity of polyol) value increased shown in Table 2. In other hands, under a constant shear rate, viscosity will generally remain almost constant, Thus, Figure 6a-c show apparent viscosity of a pseudoplastic substance increases with the decreasing their shear rate, an increase in the molecular mobility of all polyol chains (due to epoxy group were ring opened by cross-linker CaOD diol), because of increases secondary OH group and >C=C< intrinsically present in diol moiety [16-21]. The corresponding power law model indicates, the bio-polyols having higher molecular weight and it exhibits the Pseudoplastic Newtonian behavior [19,21].

3.5. Thermogravimetric analysis

The thermal stability of HSCP and HPCP polyurethanes was evaluated by thermogravimetry analysis by the heating rate 20 °C/min under the nitrogen atmosphere. The thermos-gravimetric analysis results are summarized in Table 3. The TGA curves are illustrated in Figure 7. The thermal stability of these polyurethanes an increase in the initial weight loss was observed as a result of the increase in the number of urethane groups, on the other hand, it reveals that the increase of hard segment (NCO) in both the polymers [21,22]. This is due to the increase of the aliphatic moiety HMDI and the increase of intermolecular attractions between NH and CO through H-bonding, polar-polar interaction, *etc.*, which makes the structure more compact. TGA curves of polyurethanes prepared from different polyols with different OH contents and HMDI (HSCP and HPCP) are shown in Figure 7a. The corresponding TGA curves reveal five different main degradation processes shown in Table 3.

Table 3. Formulas for varies method to calculation of kinetic parameters.

Method	Formula	Plots
Murray and White	$\int_{T_o}^{T} e^{-E^*/RT} \simeq \left(\dfrac{RT^2}{E}\right) e^{-E^*/RT}$	$\ln[\ln(1-C) - 2lnT \; vs \; \dfrac{1}{T} \; \text{for}\,(n=1)$
Coats and Redfern	$\int_{T_O}^{T} e^{\frac{-E^*}{RT}} \; dt \simeq \left(RT^2\right)\left[1 - 2\dfrac{RT}{E}\right] e^{\frac{-E^*}{RT}}$	$\log\dfrac{\left[ln(1-C)\right]}{T^2} \; vs \; \dfrac{1}{T} \; \text{for}\,(n=1)$
Doyle's	$\log\dfrac{R}{E}\int e^{\frac{-E^*}{RT}} \, dt \simeq -2.315 - 0.4567\left(\dfrac{E}{RT}\right)^{\text{for}\,20 \geq \frac{E}{RT} \geq 60}$	$\log[\ln(1-C) \; vs \; \dfrac{1}{T} \; \text{for}\,(n=1)$

Figure 6. Shear stress *vs* shear rate, shear rate *vs* viscosity plots of (a) CaOD diol, (b) SCOL polyol and (c) PCOL polyol.
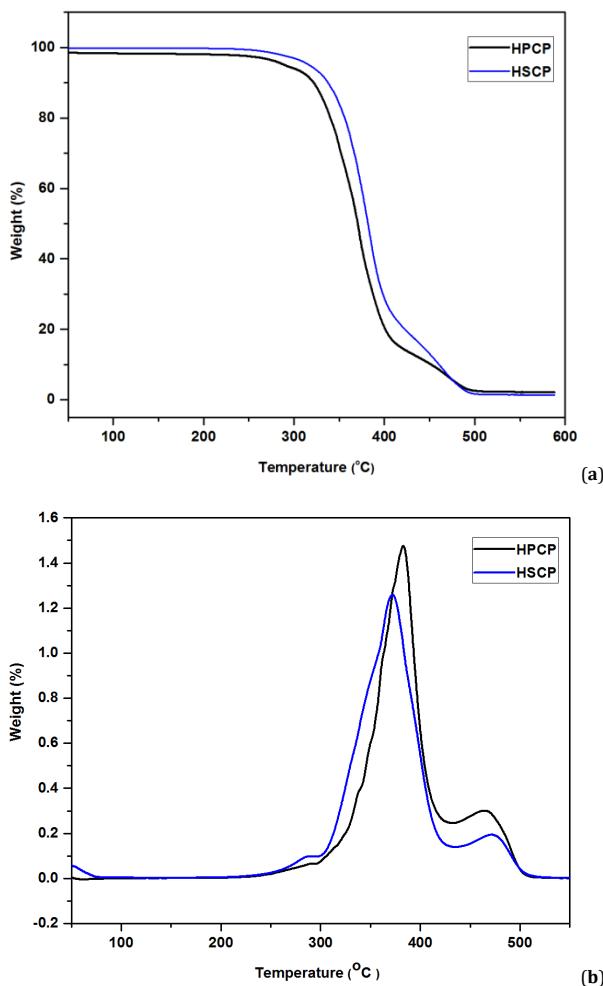
Figure 7. (a) TGA curve of HSCP and HPCP, (b) DTG curve of HSCP and HPCP.

The first degradation of the PUs was started from 250 to 310 °C corresponding to 90% weight loss (average value.) that may be due to cleavage of urethane linkages, which depend on the type of substituent present in the hexamethylene diisocyanate and polyols (SCOL and PCOL).

The second step degradation of the PUs was observed in the range of 330 to 328 °C corresponding to 88% weight loss. The thermal degradation exerted in the second step may be observed due to the breakdown of the aliphatic alkyl group of fatty acid [1-9,23]. The third step thermal degradation reported in the temperature range 380 to 392 °C and weight loss in the range of 60 to 64 % and the major weight losses between 430 to 445 °C at 37% and 450 to 495 °C at 7 to 12 % are due to complete decomposition of cross-linker this is due to sluggish amongst both PUs formulations may be presence of secondary -OH groups in castor diol moiety of SCOL and PCOL polyol. The thermograms results obtained for the aliphatic polyurethanes, and activation energy can be calculated from Figure 7a, respectively [23]. The temperature at which major decomposition started was noted as the initial decomposition temperature. The energy of activation for the major decomposition reaction steps were calculated by Murray and White, Coat's and Redfern and Doyle's methods. The aliphatic polyurethane, correct order and activation energy of the reaction were calculated graphically from Freeman-Carroll's method. (Venkatesh *et al.* were discussed for aromatic polyurethane) [20-24]. From this discussion, the aliphatic moieties of polyurethane, the cross-linking density, and

stability of the polyurethanes were calculated by Freeman-Carroll's method [23]. Activation energy can be calculated using the following approximation methods. The Arrhenius equation can be given as

$$\frac{dc}{dt} = A.e^{-E/Rt}(1-C)^n \tag{1}$$

The straight- line equation derived by Freeman and Carroll's, which is in the form of

$$\frac{\Delta \log dW/dt}{\Delta \log Wr} = n - \frac{E}{2.303 \times R} - \frac{\Delta \frac{1}{T}}{\Delta \log Wr} \tag{2}$$
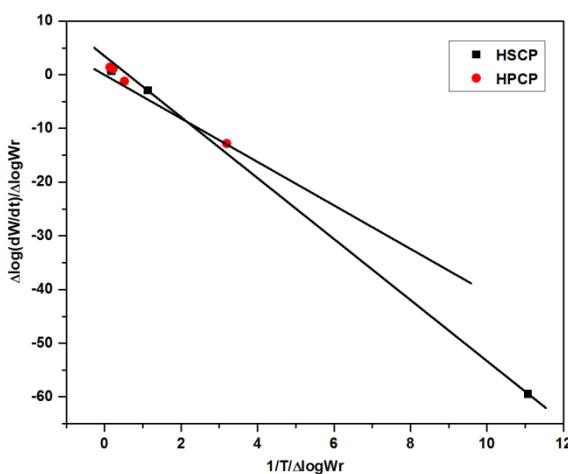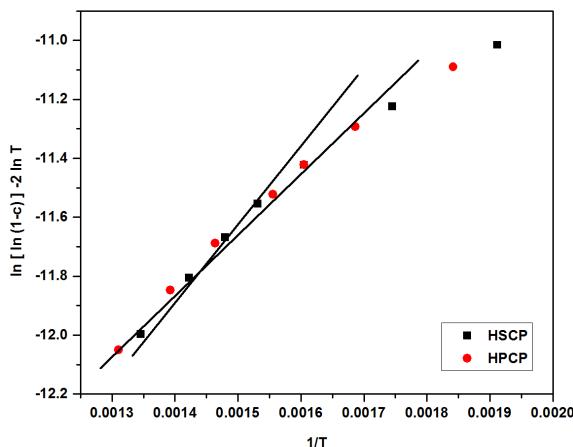
where, dW/dt = Rate of change of weight with time, W_r = Weight loss at completion of the reaction, W = Fraction of weight loss at time "t", E = Energy of activation and n = Order of reaction.

From the slope, we obtained energy of activation and intercept on y axis as order of the reaction (n = 3). Freeman and Carroll's method is plots of $A = \dfrac{\Delta \log(dw/dt)}{\Delta \log Wr}$ *vs*

$B = \dfrac{\Delta 1/T}{\Delta \log Wr}$.

Table 4. The activation energy of polyurethane calculated from different decomposition temperature.

Polymers	Temperature	Activation energy (ΔE_a) (kJ/mol)			
		Murray and White	**Coat's and Redfern**	**Doyle's**	**Freeman and Carroll**
HSCP	250	326	141	388	106
	330				
	380				
	430				
	470				
HPCP	270	346	150	439	87
	320				
	370				
	445				
	490				

Figure 8. Freeman-Carroll's curve of HSCP and HPCP.

Figure 9. Murray and White curve of HSCP and HPCP.

For the purpose of this plot dW and dWr can be determined directly from the thermogram in term of the no. of a division. The activation energy calculation from TG curves of the polyurethanes. They all presented a similar weight loss profile with the first step appearing at around 10% weight loss since the HSCP and HPCP have the same amount of urethane groups. Table 4 shows the varies weight loss and activation energies was calculated from different methods. In Figure 7b, DTG curve shows isothermal and distance between iso-conversional curves of aliphatic polyurethanes [24].
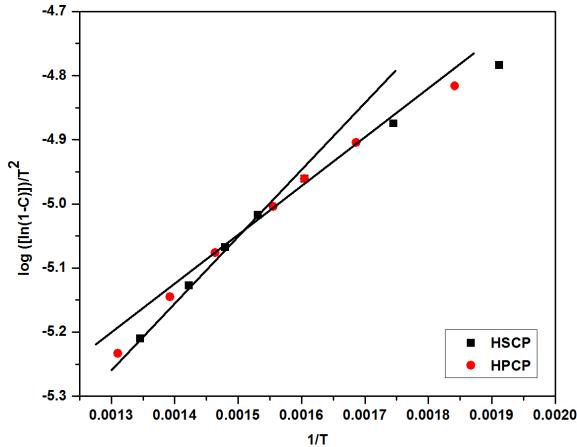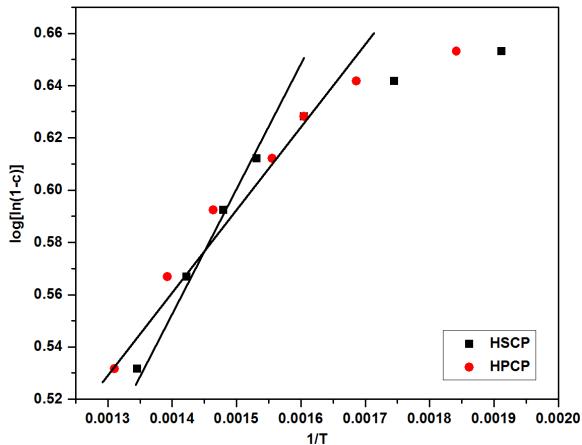
If the isothermals are fairly parallel, the activation energy does not appreciably change with temperature. However, the TGA curve of Figure 7a is demonstrating the complexity of process, when the isothermal conversion curve illustrate non-parallel irregular spacing between them. The average values of

activation energies at different iso-conversional points are calculated to be 106 and 87 kJ/mol, the estimated values are plotted and compared with those calculated using Freeman and Carroll's method (Table 4) [25-27]. From Figure 8, it is quite clear that activation energy passes through a minimum value at 50%. Figure 9, 10, and 11 shown, activation energy (HSCP and HPCP) obtained through Murray and White, Coat's and Redfern, Doyel's method is varied within 326 and 346, 141 and 150, 388 and 439 kJ/mol of the average values are shown in Table 4, while, the fluctuations in activation energy is much higher in those values obtained according to Freeman-Carroll's procedure. This large difference between the activation energy reflected the complex nature of the degradation process, which can be observed by the decrease of the activation energy with increasing conversion.

Table 5. Kinetic parameters calculated from Freeman and Carroll's method *.

Polymers	A (s^{-1})	ΔS (kcal/mol)	ΔH (kcal/mol)	ΔG (kcal/mol)	Z	S*	n	t$_f$
HSCP	1.27×10^3	10.75	-7110.49	-1418	6.18	4.36	3	1.87×10^5
HPCP	1.93×10^4	7.71	-5106.49	-1012	8.32	5.54	3	1.28×10^4

* A = Pre-exponential factor, ΔS = Entropy, ΔH = Enthalpy, ΔG = Free energy change, Z = Frequency factor, S*= Apparent entropy, n = Order of reaction (Decomposition).

Figure 10. Coat's and Redfern curve of HSCP and HPCP.

Figure 11. Doyel's curve of HSCP and HPCP.

TG analysis is commonly used to estimate thermal degradation kinetic parameters such as activation energy (E_a), pre-exponential factor (A), frequency factor (Z), apparent entropy (S*) and reaction order (n) [25-28]. Kinetic constants of polyurethane (HSCP and HPCP) measured at heating rates of 5 to 20 °C/min indicates that at larger heating rates both the activation energy and the pre-exponential factor decreases. Using a different decomposition temperature one-step kinetic model the order of reaction was found to be approximately 3.0, the enthalpy, entropy and free energy change calculated from Freeman and Carroll's method. The activation energy of polyurethanes namely HSCP and HPCP was calculated, the corresponding approximate values are 106 and 87 kJ/mol and the pre-exponential factor value are 1.27×10^3 and 1.93×10^4 s^{-1} [25]. Based on these results we suppose that the different kinetics degradation observed in our study is related to the different fatty acid composition of the sesame –polyol, and peanut-polyol, i.e., the presence of cross-linker CaOD diol and epoxy groups. We observe an excellent fit for the main part of the exotherm corresponding to more than 70% of the surface. Table 5 indicates that the molar enthalpy of urethane formation from secondary hydroxyl groups and aliphatic isocyanates is 10.75 and 7.71 kJ/mol [5,8,23,27]. From those

results, we can consider that, for HMDI, the two different polyurethanes have an equal molar enthalpy of reaction at lower than 298 K. The reaction rates are sufficiently slow to allow efficient mixing during a few minutes without the significant extent of reaction.

3.6. Lifetime prediction

The solid-state thermal mechanism and kinetics of sesame and peanut oil-based polyurethanes, to improve their chain mobility and processability of chain extender (HMDI). Thus, in this discussion, (the apparent kinetic parameters calculated from this study have been used to obtain the lifetime of formulated vegetable oil- based polyurethane systems) the estimated lifetime of a polyurethane until failure has been defined as the time when the mass loss reaches 7 and 4 wt % (HSCP and HPCP).

Following equation can be estimated for lifetime of the polymer.

$$\frac{d\alpha}{dt} = A.\exp\frac{E_a}{RT}\left(1-a\right)^n \tag{3}$$

$$t_f = \frac{1-0.0513}{A}\exp\frac{E_a}{RT}\left(n=1\right) \tag{4}$$

The obtained approximate activation energy (form Freeman and Carroll's) of HSCP and HPCP, 106 and 87 kJ/mol. In the polymeric chain mobility between C=O and NH, the dissociation energy is lesser due to the five different mass losses obtained from the TGA curve, which could be easy to find out the lifetime prediction of the polymers (lifetime was strongly dependent on the service temperature, and decreased significantly as the temperature increases from 25 to 600 °C) which shown in Table 5. In decomposition, the temperature supplies energy to increase chain mobility and rate of degradation, while shortening its lifetime [26,27]. However, the kinetics of the degradation process depends strongly on chain mobility, which further depends on the physical state of the polymer [27-31]. Chain mobility is much higher in the molten state than in solid state, thereby making the predictions even inaccurate for the solid state.

4. Conclusion

The primary objective of this discussion is to develop the vegetable oil based polyols, which is a promising alternative of chemically synthesized polyurethanes. In this present study, sesame and peanut oil-based polyurethanes have been successfully synthesized. The activation energy and lifetime prediction calculated from TG curves of the polyurethanes. The average values of activation energies at different iso-conversion points are calculated to be 106 and 87 kJ/mol, the estimated values are calculated using Freeman and Carroll 's method. The ΔE obtained through Murray and white method is varied within 326 and 346, 141 and 150, 388 and 439 kJ/mol of the average value, while, the fluctuations in activation energy is much higher in those values obtained according to Freeman and Caroll's procedure. This large difference between the activation energy reflected the complex nature of the degradation process, which can be observed by the decrease of the activation energy with increasing conversion. The

segmental ratio has a significant effect on the thermal properties of both aliphatic polyurethanes. This is due to the increase of the aliphatic moiety HMDI and an increase of intermolecular attractions between NH and CO through H-bonding, polar-polar interaction, *etc.*, which makes the structure more compact. The obtained approximate activation energy (form Freeman and Carroll's) of HSCP and HPCP values to determine the lifetime of the polymers (HSCP is 1.87×10^5 and HPCP is 1.28×10^4). In the polymeric chain mobility between C=O and NH, the dissociation energy is lesser due to the five different mass losses obtained from the TGA curve. In decomposition, the temperature supplies energy to increase chain mobility and rate of degradation, while shortening its lifetime. However, the kinetics of the degradation process depends strongly on chain mobility, which further depends on the physical state of the polymers (HSCP and HPCP). Chain mobility is much higher in the molten state than in solid state, thereby making the predictions even inaccurate for the solid state. The resultant polyurethanes which can be used as coating, adhesives, foams, biomedical, battery and sensor applications.

Disclosure statement DS

Conflict of interests: The authors declare that they have no conflict of interest.
Author contributions: All authors contributed equally to this work.
Ethical approval: All ethical guidelines have been adhered.
Sample availability: Samples of the compounds are available from the author.

ORCID iD

Venkatesh Desappan
iD http://orcid.org/0000-0001-9005-6494
Jaisankar Viswanathan
iD http://orcid.org/0000-0003-0894-4703

References

[1]. Morral-Ruiz, G.; Melgar-Lesmes, P.; Solans, C.; Garcia-Celma, M. J. Advanced Polyurethane Biomaterials, 1st Edition, Elsevier, 2016, pp. 195-216.

[2]. Francolini, I.; Piozzi, A. Advanced Polyurethane Biomaterials, 1st Edition, Elsevier, 2016, pp. 349-385.

[3]. Boffto, M.; Sartori, S.; Mattu, C.; Ciardelli, G. Advanced Polyurethane Biomaterials, 1st Edition, Elsevier, 2016, pp. 387-416.

[4]. Zhang, C.; Madbouly, S. A.; Kessler, M. R. *Appl. Mater. Interf.* **2015**, *7*, 1226-1233.

[5]. Chen, R.; Zhang, C.; Kessler, M. R. *J. Appl. Poly. Sci.* **2015**, *132(1)*, 41213, 1-10.

[6]. Zhang, J.; Tang, J. J.; Zhang, J. X. Inter. *J. Poly. Sci.* **2015**, *1,* 529-535.

[7]. Dai, H.; Yang, L.; Lin, B. , Wang, C.; Shi, G. *J. Am. Oil Chem. Soc.* **2009**, *86*, 261-267.

[8]. Tenorio-Alfonso, A.; Sanchez, M. C.; Franco, J. M. *J. Poly. Sci.* **2017**, *9*, 132-146.

[9]. Musa, I. A. *Egyp. J. Petrolium* **2016**, *25*, 21-31.

[10]. Miao, S.; Zhang, S.; Zhiguo, S.; Wang, P. *J. App. Poly. Sci.* **2012**, *127*, 1929-1936.

[11]. Mungroo, R.; Pradhan, N. C.; Goud, V. V.; Dalai, A. K. *J. Am Oil Chem. Soc.* **2008**, *85*, 887-896.

[12]. Gurunathan, T.; Rao, C. R. K.; Narayan, R.; Raju, K. *J. Mat. Sci.* **2013**, *48*, 67-80.

[13]. Petrovic, Z. S.; Yang, L.; Zlatanic, A.; Zhang, W.; Javni, I. *J. Appl. Poly. Sci.* **2007**, *105*, 2717-2727.

[14]. Caillol, S.; Desroches, M.; Boutevin, G.; Loubat, C. D.; Auvergne, R. M.; Boutevin, B. *Eur. J. Lipid Sci. Tech.* **2012**, *114*, 1447-1459.

[15]. Zhang, C.; Xia, Y.; Chen, R.; Kessler, M. R. *ACS Sus. Chem.* **2014**, *2*, 2465-2476.

[16]. Meier, M. A.; Metzger, J. O.; Schubert, U. S. *Chem. Soc. Rev.* **2007**, *36*, 1788-1802.

[17]. Arniza, M. Z.; Hoong, S. S.; Idris, Z.; Yeong, S. K.; Hassan, H. A.; Din, A. K.; Choo, Y. M. *J. Am. Oil Chem. Soc.* **2015**, *92*, 243-255.

[18]. Rajendran, T. V.; Jaisankar, V. *J. Mat. Sci.* **2015**, *2*, 4421-4428.

[19]. Zhang, C.; Xia, Y.; Chen, R.; Huh, S.; Johnston, P. A.; Kessler, M. R. *ACS Sus. Chem.* **2013**, *152*, 1477-1484.

[20]. Okieimen, F. E.; Bakare, O. J.; Okieimen, C. O. *Ind. Crops Prod.* **2002**, *15(2)*, 139-144.

[21]. Lozada, Z.; Suppes, G. J.; Tu, Y. C.; Hsieh, F. H. *J. App. Poly. Sci.* **2009**, *113*, 2552-2560.

[22]. Thakur, S.; Karak, N. *Prog. Org. Coat.* **2013**, *76*, 157-164.

[23]. Kong, X.; Liu, G.; Curtis, J. M. Inter. *J. Adhesion Adhesives* **2011**, *31*, 559-564.

[24]. Gurnule, W. B.; Thakre, M. B. *J. Phar. Bio. Chem. Sci.* **2014**, *5(2)*, 204-213.

[25]. Venkatesh, D.; Jaisankar, V. *Inter J Sci. Eng. Invest.* **2018**, *7(73)*, 44-51.

[26]. Mallakpour, S.; Taghavi, M. *Iran. Poly. Jour.* **2009**, *18(11)*, 857-872.

[27]. Khan, M. I.; Azizli, K.; Sufian, S.; Man, Z.; Khan, A. S. *RSC Adv.* **2015**, *5*, 20788-20799.

[28]. Jing, H.; Chen, M.; Tian, H.; Deng, W. *RSC Adv.* **2015**, *5*, 81134- 81141.

[29]. Basta, A.; Missori, M.; Girgis, A. S.; Spirito, M.D.; Papi, M.; El-Saied, H. *RSC Adv.* **2014**, *4*, 59614-59625.

[30]. Mustapa, S. R.; Aung, M. M.; Ahmad, A.; Mansor, A.; Tiankhoon, L. *Electrochim. Acta* **2016**, *222*, 293-302

[31]. Othaman, M. B. H.; Ahmad, Z.; Osman, H.; Omar, M. F.; Akil, H. M. *RSC Adv.* **2015**, *5*, 92664-92676.